

# Investigation of the Effects of Facility Background Pressure on the Performance and Voltage-Current Characteristics of the High Voltage Hall Accelerator

Hani Kamhawi<sup>\*</sup>, Wensheng Huang<sup>†</sup>, Thomas Haag<sup>‡</sup>,  
*NASA Glenn Research Center, Cleveland, Ohio, 44135*

and

Rostislav Spektor<sup>§</sup>  
*The Aerospace Corporation, El Segundo, California, 90245*

The National Aeronautics and Space Administration (NASA) Science Mission Directorate In-Space Propulsion Technology office is sponsoring NASA Glenn Research Center to develop a 4 kW-class Hall thruster propulsion system for implementation in NASA science missions. A study was conducted to assess the impact of varying the facility background pressure on the High Voltage Hall Accelerator (HiVHAc) thruster performance and voltage-current characteristics. This present study evaluated the HiVHAc thruster performance in the lowest attainable background pressure condition at NASA GRC Vacuum Facility 5 to best simulate space-like conditions. Additional tests were performed at selected thruster operating conditions to investigate and elucidate the underlying physics that change during thruster operation at elevated facility background pressure. Tests were performed at background pressure conditions that are three and ten times higher than the lowest realized background pressure. Results indicated that the thruster discharge specific impulse and efficiency increased with elevated facility background pressure. The voltage-current profiles indicated a narrower stable operating region with increased background pressure. Experimental observations of the thruster operation indicated that increasing the facility background pressure shifted the ionization and acceleration zones upstream towards the thruster's anode. Future tests of the HiVHAc thruster are planned at background pressure conditions that are expected to be two to three times lower than what was achieved during this test campaign. These tests will not only assess the impact of reduced facility background pressure on thruster performance, voltage-current characteristics, and plume properties; but will also attempt to quantify the magnitude of the ionization and acceleration zones upstream shifting as a function of increased background pressure.

---

<sup>\*</sup> Research Engineer, In Space Propulsion Systems Branch, hani.kamhawi-1@nasa.gov.

<sup>†</sup> Research Engineer, In Space Propulsion Systems Branch, wensheng.huang@nasa.gov.

<sup>‡</sup> Propulsion Engineer, In Space Propulsion Systems Branch, thomas.w.haag@nasa.gov.

<sup>§</sup> Section Manager Electric Propulsion and Plasma Sciences, Propulsion and Mechanics Dept., Rostislav.Spektor@aero.org.

## I. Introduction

**E**lectric propulsion (EP) systems performance can significantly reduce launch vehicle requirements, costs, and spacecraft mass because of its high specific impulse capability when compared to chemical propulsion. Electric propulsion systems enhance NASA's ability to perform scientific space exploration and can enable new science missions. NASA science missions to small bodies include fly-by, rendezvous, and sample return from a diverse set of targets. For example, NASA has successfully employed EP systems in the Deep Space 1 (DS1) and Dawn missions.<sup>1,2,3</sup> To augment its capability to perform these and other solar system exploration missions, NASA continues to develop advanced EP technologies.<sup>4</sup> Recent small body mission studies indicate that the majority of these small body missions are enabled by the use of EP, and nearly all of the small body missions of interest are enhanced with EP.<sup>5</sup>

NASA Science Mission Directorate (SMD) In-Space Propulsion Technology (ISPT) Project funds new EP system development for future NASA science missions.<sup>6</sup> The two primary EP elements of this project are the development of NASA's Evolutionary Xenon Thruster (NEXT) ion thruster propulsion system<sup>7</sup> for NASA Discovery, New Frontiers and Flagship-class missions and the development of a long-life High Voltage Hall Accelerator (HiVHAc) as a lower cost EP option for NASA Discovery-class science missions.

In addition to the mission performance benefits that can be realized with EP systems, significant cost savings can be achieved by use of Hall system when compared to gridded ion and chemical propulsion systems.<sup>8</sup> The Hall thruster system option will not only enable a wide range of Discovery-class missions but will enable science return far greater than the chemical alternatives.<sup>9</sup>

Previous studies and investigations have found that the facility background pressure environment affects thruster performance, a summary of several studies was presented in Reference 10. Studies on the SPT-100 thruster have shown that facility background pressures below  $5 \times 10^{-5}$  Torr are sufficient for reliable performance data, whereas background pressures below  $1.3 \times 10^{-5}$  Torr were needed for plume measurements 1.2 m from the thruster.<sup>11</sup> Recent study performed at The Aerospace Corporation, characterized the operation of a 500 W class thruster at various background pressure conditions. The study found that the discharge became less stable with increased background pressure and that ingested neutrals increased the amplitude of the breathing mode oscillations.<sup>12</sup>

As part of maturing the HiVHAc thruster and system hardware, the performance of the HiVHAc thruster was assessed in an environment that is as close as possible to a space-like environment. This included operating the thruster in as low as possible background pressure conditions. This paper is focused on assessing the performance and stability of the thruster in the lowest attainable background pressure conditions at NASA GRC. This paper does not address the effect of the background pressure on the discharge erosion zone location or erosion rates. This paper details recent tests HiVHAc engineering development unit 2 (EDU), thereafter referred to as EDU, at the NASA GRC vacuum facility 5 (VF5). The test performed at GRC's VF5 attained the lowest background pressure conditions, during thruster operation, than any previous tests of the HiVHAc thruster. In addition, evaluation and of the HiVHAc thruster performance at selected thruster throttle points and a comprehensive voltage-current (V-I) characterization of the HiVHAc thruster was performed at background pressure conditions that are three and ten times higher than the lowest background pressure test conditions attained in VF5.

This paper is organized as follows: Section II presents the experimental apparatus used in this test campaign. Section III presents the experimental results. Section IV presents a discussion of the experimental results. Section V presents conclusions and future test plans.

## II. Experimental Apparatus

The HiVHAc thruster facility background pressure sensitivity investigation was performed at NASA GRC's VF5. The major HiVHAc sub-system components that were employed during the test were:

- The HiVHAc EDU thruster which has undergone extensive performance and thermal characterizations tests in addition to undergoing a random vibration test.<sup>13</sup> The EDU thruster is designed to operate at a peak discharge power of 3.9 kW and at discharge voltages up to 650 V. The thruster incorporates an in-situ discharge channel replacement mechanism for life extension. The thruster development plan has been reported earlier;<sup>13</sup>
- The Colorado Power Electronics (CPE) brassboard (BB) power processing unit (PPU), designated BB 1 PPU;<sup>14,15</sup>
- A 15 kW 600 V capable power supply that was remotely operated with control software created by The Aerospace Corp., and

- Two laboratory xenon feed systems.

The BB 1 PPU was placed outside VF5 to preserve the ability to perform V-I characterization of the HiVHAc thruster using the laboratory high voltage power supply. Figure 1 shows a picture of the HiVHAc thruster hardware setup.

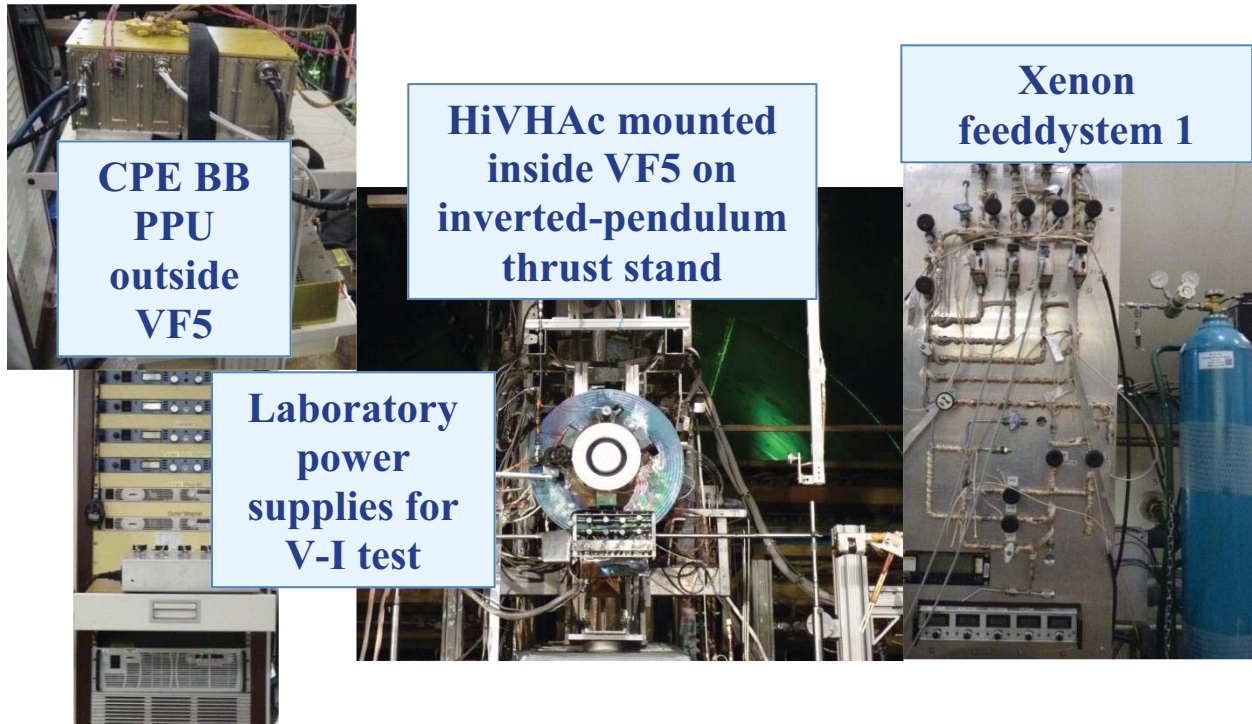


**Figure 1. HiVHAc thruster test hardware.**

#### **A. Vacuum Facility 5**

The main chamber of VF5 is 4.6 m in diameter and is 18.3 m long. VF5's main port (designated E55) is 1.8 m in diameter and is 2.5 m long. VF5 can be evacuated with cryopanel and oil diffusion pumps. For this test campaign the HiVHAc thruster was placed in VF5's main volume at the facility midsection facing away from the facility cryopanel. That was done to assure that the lowest possible background pressure conditions were attained during thruster operation. Figure 2 shows a picture of the HiVHAc thruster mounted inside VF5. Facility pressures were monitored with four ion gauges, three of which were mounted next to the thrust stand, fourth being on the facility south chamber wall. Manufacturer specifications state that the ion gauges are accurate to  $\pm 6\%$  of reading. The location of the gauges is shown in Fig. 2 and is approximately 1 m from the thruster. Ion gauges 1 and 2 are both facing downstream while ion gauge 3 is facing upstream. Ion gauge 1 and 2 agree to within 10% of each other. Ion gauge 3 reports 0.63 to 0.72 times the reading as ion gauge 2. Ion gauge 2 readings were used to determine the number of multiples of the lowest achievable background pressure that the thruster was experiencing. All reported ion gauge readings are corrected for xenon.

#### **B. Laboratory Propellant Feed Systems**

Two laboratory propellant feed systems were used in the HiVHAc pressure sensitivity test. Feed system 1, supplied xenon to the thruster and the cathode assembly. The propellant feed system 1 utilized four mass flow controllers (MFCs). A 200 sccm MFC was used to supply xenon to the VACCO XFCM unit (was not used in this test). A 100 sccm MFC supplied xenon to the thruster discharge. For the cathode, a 10 sccm MFC unit was used. Laboratory feed system 2, not shown, employed 3 MFCs, a 1 SLM, a 500 SCCM, and 200 SCCM controllers. The MFCs were used to supply xenon to raise the facility background pressure. Only feed system 1 MFCs were calibrated before and

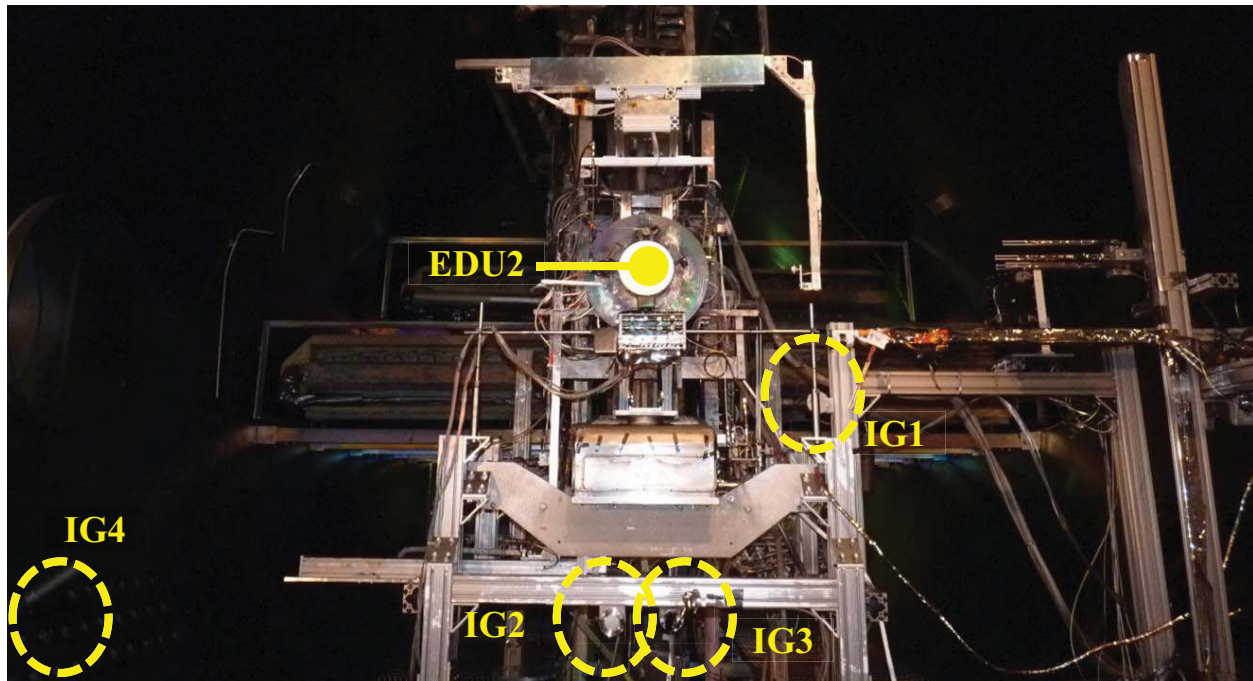


**Figure 2. The HiVHAc EDU thruster mounted on the inverted pendulum thruster stand inside VF5, denoted on the photograph are the locations of the 4 ion gauges that were used to monitor the pressure in the vicinity of the thruster.**

after the test. The MFC calibration curves indicated that the anode and cathode flow rates uncertainty is  $\leq 1\%$  of set value.

#### **C. Power Console**

For this test campaign the thruster was mostly powered with the CPE BB PPU, shown in Fig. 1. The CPE BB PPU was placed outside the vacuum chamber to allow for use of a laboratory power supply during thruster V-I characterization tests. The BB PPU has demonstrated over 2,000 hours of operation in vacuum as was reported earlier.<sup>15</sup> The PPU is powered with a 0-160 Vdc 90 A power supply. The operation of the CPE BB PPU is controlled with a control console built by CPE. The high-voltage laboratory power supply that was used during V-I tests is a 15 kW 600 V capable power supply.

#### **D. Inverted Pendulum Thrust Stand**

A null-type water-cooled inverted pendulum thrust stand was implemented during thruster performance evaluation. The power cables were fed from the vacuum feed thru to the thruster using a “water fall” configuration to minimize the thermal drift of the thrust stand readings. In-situ thrust stand calibrations were performed prior, during, and after thruster testing. In addition, during testing the thruster was periodically turned off to measure the thrust stand thermal drift magnitude, and the corrections were incorporated in the reported thrust. Thrust measurement uncertainty was estimated at 2% of the measured value.

#### **E. Data Acquisition**

A data logger was used to measure and record the thruster operating parameters. The measurements were calibrated using a calibrated meter and they included the various thruster operating currents, operating voltages, thruster component temperatures, and facility pressure in the vicinity of the thruster.

#### **F. Diagnostics**

An extensive set of diagnostics was acquired to take full advantage of the opportunity to test HiVHAc EDU in VF5. These diagnostics included:

- Plasma diagnostics included a near-field Faraday probe that was mounted on an axial stage and rotary stage, far-field retarding potential analyzer (RPA),  $E \times B$ , and Langmuir probes. Results from the Faraday, RPA,  $E \times B$ , and Langmuir probes were reported by Huang *et al.*<sup>16</sup> In addition to the above diagnostics, an Air Force Research Laboratory (AFRL) high speed Langmuir probe (HSLP) rake was



implemented in this test.<sup>17</sup> Analysis of the HSLP data is reported in a companion paper by Huang *et al.*,<sup>18</sup>

- Fast camera imaging of the HiVHAc thruster discharge was performed using a FAST camera. Analysis of the FAST CAM images is reported in a companion paper by Huang *et al.*,<sup>18</sup>
- Type-K thermocouples were used to monitor the temperature of various thruster components during this test campaign. Analysis of the results is on-going and will be presented at a later time; and
- Infrared camera imaging of the HiVHAc thruster using a FLIR Aerospace camera that was placed inside a pressurized enclosure inside VF5 4 m away from the thruster. Results from the thermocouple and IR camera measurements will also be presented a later time.

Figure 3 shows a picture of the various diagnostics used during this test campaign. The results from the thermocouple readings, and the IR camera images are still being analyzed and will be reported in future publications.

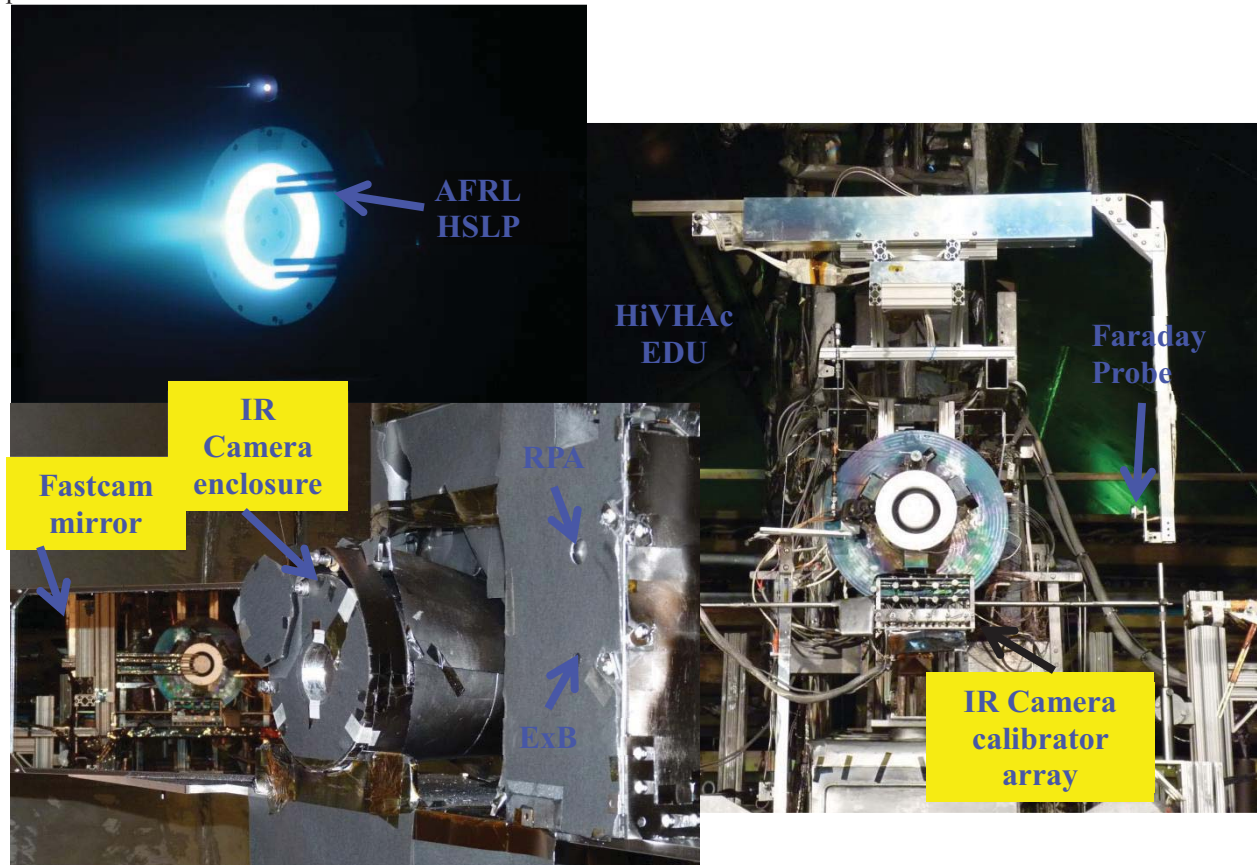


**Figure 3. Photograph showing the various diagnostics implemented during the HiVHAc thruster test campaign at NASA GRC's VF5**

### III. Experimental Results

This section has three sub-sections. In section IIIA, the performance evaluation of HiVHAc EDU for the entire throttle operating conditions is presented and compared to results from the performance acceptance test (PAT) that were reported in 2012.<sup>13</sup> In Section IIIB, results from a pressure sensitivity study that was performed at 7 throttle conditions are presented. Finally, Section IIIC presents the V-I profiles that were acquired at different facility background conditions for different thruster anode flow rates and electromagnet currents.

#### A. Performance Characterization

The HiVHAc EDU thruster performance was characterized for the thruster's entire throttle range in VF5. The thruster performance was evaluated for discharge voltages between 200 and 650 V. Table 1 below lists the thruster operating condition where the thruster performance was characterized. For the thruster performance

characterization, BB 1 and laboratory XFS were used. Although the performance acceptance test (PAT) of the HiVHAc thruster was performed in April/May of 2012 at NASA GRC's VF12, the tests performed in VF5 were performed at background pressure levels that are approximately 6-7 times lower than during the PAT in VF12.<sup>13</sup>

**Table 1. HiVHAc EDU2 thruster performance characterization test throttle operating conditions.**

V <sub>d</sub> , V	Discharge Power, W								
	300	500	1000	1,500	2,000	2,500	3,000	3,500	3,900
200	•	•	•	•					
300		•	•	•	•				
400			•	•	•	•	•		
500			•	•	•	•	•	•	•
600				•	•	•	•	•	•
650				•	•	•	•	•	•

For this test campaign, VF5 was equipped with four ion gauges that were positioned in close proximity to the thruster, shown previously in Fig. 2.

The discharge specific impulse and thrust efficiency of the thruster were calculated using

$$(I_{sp})_d = \frac{T}{\dot{m}_a g} \quad \text{and} \quad (\eta_t)_d = \frac{T^2}{2\dot{m}_a P_d} \quad (1) \text{ and } (2)$$

Total specific impulse and efficiency were calculated using

$$I_{sp} = \frac{T}{(\dot{m}_a + \dot{m}_c)g} \quad \text{and} \quad \eta_t = \frac{T^2}{2(\dot{m}_a + \dot{m}_c)P_{Total}} \quad (3) \text{ and } (4)$$

where  $P_{Total}$  includes the discharge, electromagnet, and cathode keeper power. For the total performance results that will be reported herein, the electromagnet power used in the calculation is based on thruster electromagnet voltage when it is at steady state temperature. This assures that we are accounting for the highest magnet power in the thruster's total efficiency calculation.

For the EDU thruster, Fig. 5 presents the discharge specific impulse (left) and discharge efficiency (right) profiles, whereas, Fig. 6 presents the total specific impulse (left) and thrust efficiency (right) profiles. Test results indicate performance levels that are lower than levels demonstrated during the performance acceptance test (PAT) of EDU in VF12.<sup>13</sup> Table 2 below summarizes the HiVHAc EDU thruster performance in VF5 and VF12 at selected operating points. Figure 7 presents the discharge specific impulse (left) and efficiency (right) for the VF5 and VF12 tests for HiVHAc EDU thruster operation at discharge voltages of 300, 500, and 650 V.

Results in Table 2 and Fig. 7 show that the thruster performance in VF12, at elevated background pressure conditions, was consistently higher than its performance in VF5. Results in Table 2 and Fig. 7 show that the greatest performance drop occurred at discharge voltages of 600 and 650 V at 3.9 kW (excluding performance change at 200 V). To elucidate the reasons behind the performance decrease in the HiVHAc thruster operation during the VF5 tests, further analysis of the experimental data is performed and presented later in this section. Figure 8 presents a plot of the VF5 and VF12 facility pressure (on log scale) near the thruster as a function of the total injected flow (includes anode and cathode flows). The pressure readings in VF5 and VF12 were taken approximately the same radial distance from the thruster exit plane. A linear curve fit was applied to the experimental data (Pressure vs. injected flow). In general, the background pressure conditions during the VF5 test were approximately 6 times lower than their values during the VF12 test.

The ingested flow amount is estimated by  $\frac{n\bar{c}}{4}A\eta_c$ , where  $n$  is the number density (calculated from facility pressure),  $\bar{c}$  is the average thermal speed,  $A$  is the thruster open exit area, and  $\eta_c$  is the Clausing factor. For this simplified analysis and to estimate the highest possible value for the ingested flow a Clausing factor of 1 is used. Estimates of the ingested flow indicate that for VF5 and at the highest operating facility background pressure, the ingested flow only contributes an additional 0.05% of the total injected flow. For VF12 and for the highest operating background pressure, the ingested only contributes an additional 0.3% of the total injected flow. This simplified analysis indicates that for thruster operation in both VF5 and VF12, the ingested flow amounts (relative to total

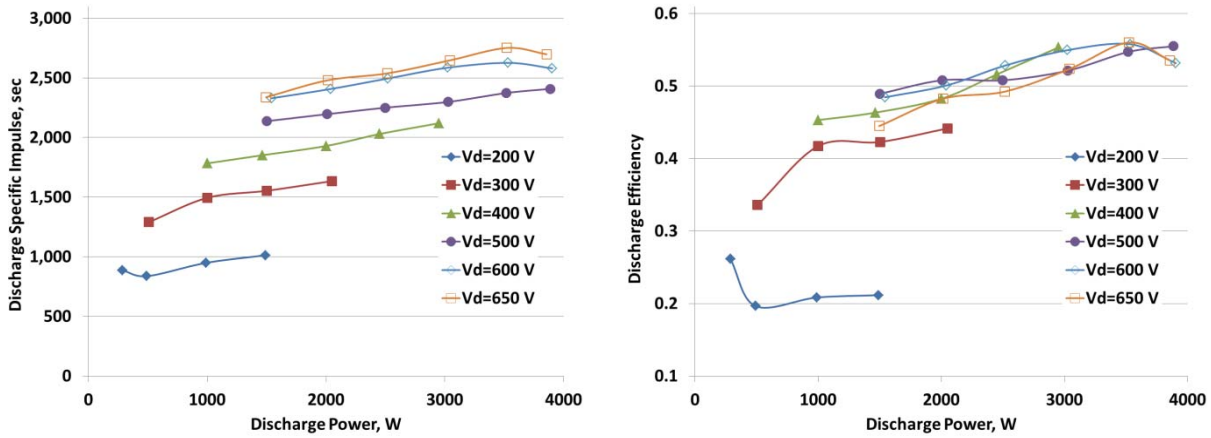


Figure 5. Discharge specific impulse profiles for the HiVHAc EDU 2 thruster for discharge voltages between 200 and 650 V during tests at NASA GRC's VF5.

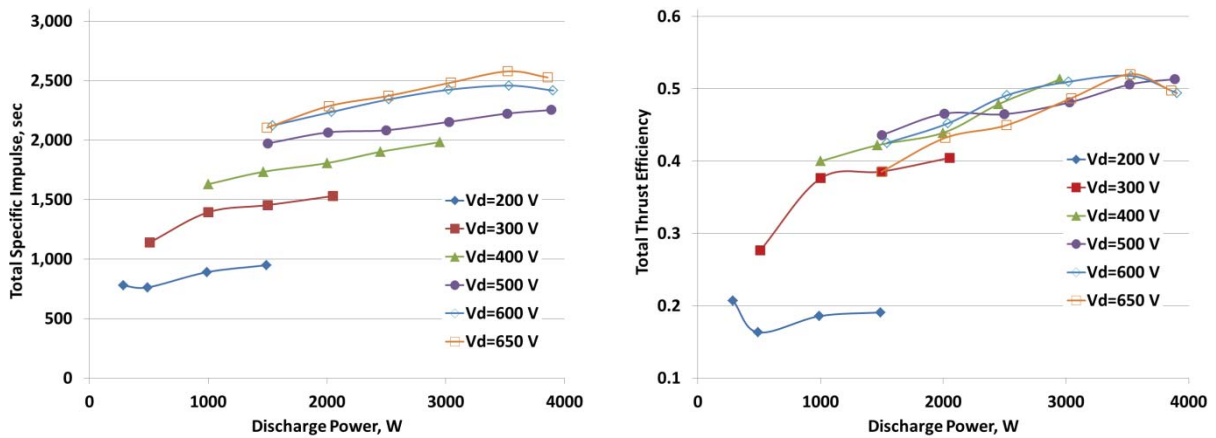
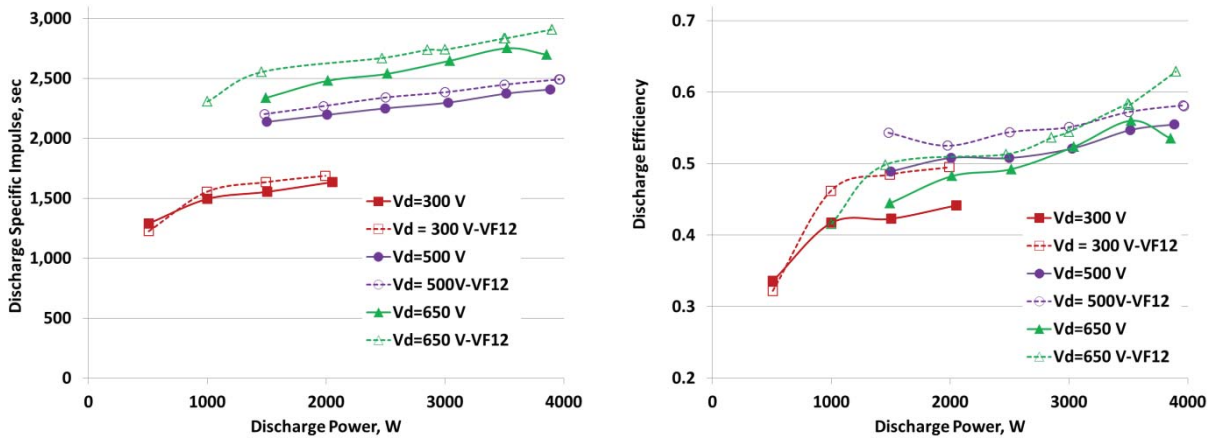


Figure 6. Total specific impulse profiles for the HiVHAc EDU thruster for discharge voltages between 200 and 650 V during tests at NASA GRC's VF5.

Table 2. HiVHAc EDU thruster discharge performance in VF5 and VF12 at selected operating conditions, VF 5 discharge specific impulse uncertainty is  $\pm 3\%$  and discharge Efficiency uncertainty is  $\pm 7\%$ , and VF12 discharge specific impulse uncertainty is  $\pm 2\%$  and discharge Efficiency uncertainty is  $\pm 5\%$

Discharge Voltage, V	Discharge Power, W	$I_{sp,d}$ , sec		$\eta_d$	
		VF5	VF12	VF5	VF12
200	1,000	945	1,115	0.19	0.34
300	1,500	1,553	1,634	0.42	0.49
400	2,000	1,929	2,031	0.48	0.55
400	3,000	2,120	2,106	0.55	0.56
500	3,000	2,299	2,384	0.52	0.55
500	3,500	2,373	2,447	0.55	0.57
500	3,900	2,407	2,490	0.55	0.58
600	3,000	2,585	2,749	0.55	0.61
600	3,500	2,626	2,718	0.56	0.61
600	3,900	2,580	2,757	0.53	0.62
650	3,000	2,647	2,739	0.52	0.54
650	3,500	2,751	2,833	0.56	0.58
650	3,900	2,698	2,906	0.54	0.63



**Figure 7. Discharge specific impulse (left) and efficiency (right) profiles for the HiVHAc EDU 2 thruster for discharge voltages of 300, 500, and 650 V during tests at NASA GRC's VF5 and VF12.**

injected xenon flow) are not substantial enough to greatly impact the thruster discharge current and performance to the levels that were measured herein. There is large uncertainty in the actual area where ingestion occurs due to discharge extending beyond the thruster's exit plan, however, an increase of a factor of two to three times in the ingestion area still does not account for the change in thruster performance due to operation at higher background pressure conditions.

To gain further insights into why HiVHAc EDU thruster performance decreased when tested in VF5, Fig. 9 presents the thruster anode flow rate as a function of thruster discharge current for thruster operation at discharge voltages of 300, 500, and 650 V for both VF5 and VF12 tests. Results in Fig. 9 indicate that at 300 V and for a given discharge current, the flow rate required to attain a specific discharge current was higher in VF12 than in VF5, although the ingested flow magnitudes are higher in VF12 when compared to VF5 due to VF12's elevated background pressure. For 500 and 650 V thruster operation, an opposite trend was observed. A lower flow rate was necessary to achieve a specific discharge current in VF12 when compared to VF5. This would be expected since the ingested flow fraction in VF5 is lower than in VF12 due to the lower facility background pressure. For 500 and 650 V thruster operation, as is shown in Fig. 9, an additional 2-5% xenon flow was required in VF5 to attain the same discharge current as VF12. This additional flow amount cannot be entirely explained by the higher amounts of ingested flow in VF12 when compared to VF5. This indicates that the HiVHAc EDU thruster operation in VF5 was different than in VF12, operation in a pressure environment that is approximately six times lower is suspected to result in a fundamental change in the location of the thruster's ionization and acceleration zones and how the cathode couples to the thruster.

Figure 10 presents a plot of thrust as a function of anode flow rate for thruster operation at 300, 500, and 650 V in VF5 and VF12. Results in Fig. 10 indicate that at 300 V higher thrust was achieved in VF12 than in VF5 mainly due to the higher flow rates that were needed to achieve the same discharge current. However, at 500 and 650 V, the thrust magnitudes in VF12 tests were higher than VF5 although lower anode flow rates were needed to achieve the same discharge current. A fraction of this improved performance could be attributed to flow ingestion, but results indicate that there is evidence that other aspects of the thruster operation have changed due to the increased facility background pressure as is discussed in the Section 4.

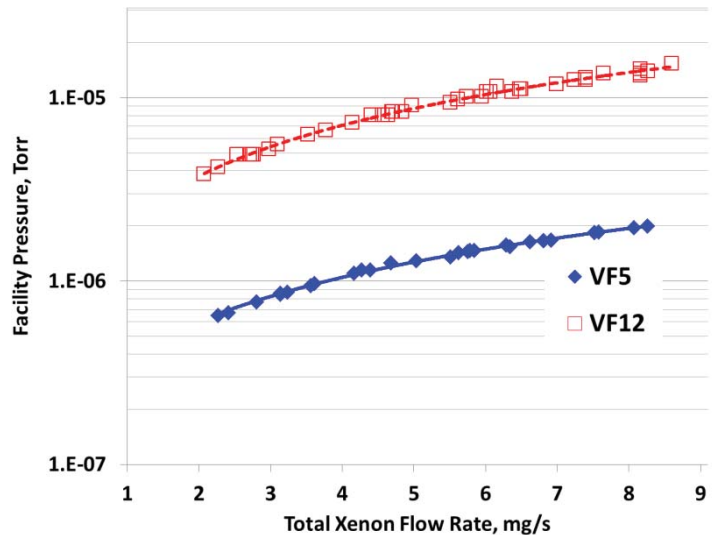


**Figure 8. VF5 and VF12 facility pressure as function of total injected xenon flow rate**



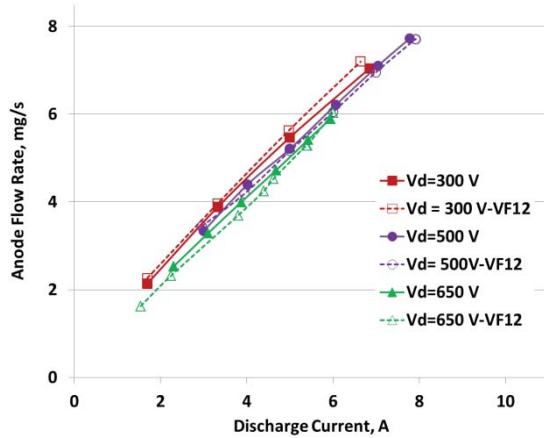


Figure 9. VF5 and VF12 HiVHAc EDU anode flow rate as a function of thruster discharge current for 300, 500, and 650 V operation.

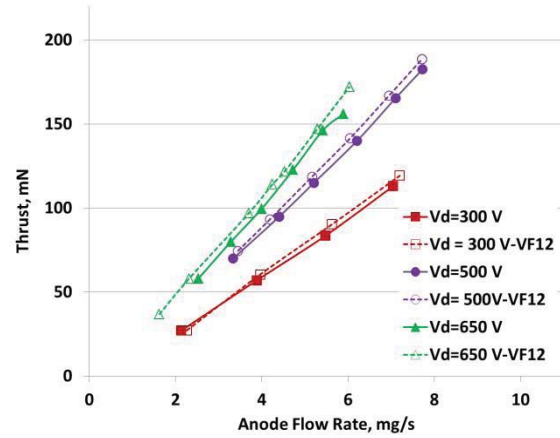


Figure 10. VF5 and VF12 HiVHAc EDU thrust as a function of anode flow rate for 300, 500, and 650 V operation.

### B. Vacuum Facility 5 Pressure Sensitivity Characterization

To further investigate the effect of facility background pressure on the HiVHAc EDU thruster operation and performance, additional tests were performed in VF5. These additional tests included testing the thruster at discharge voltages of 300, 400, and 500 V. Table 3 summarizes the thruster test conditions during the pressure sensitivity test. For all test conditions (except 500 V and 2 kW), the facility pressure was increased to approximately three and ten times the lowest possible achievable pressure for the given test condition. Ion gauge 2 readings (located at the thruster's exit plane below the thruster, see Fig. 2) were used during this investigation. The facility pressure was elevated by injecting xenon (from feed system #2) 4 m downstream of the thruster's exit plane toward the facility endcap (away from the thruster). Table 3 presents the lowest facility background pressures that were achieved for the various test conditions. Testing at discharge voltages above 500 V was attempted but was not successful due to glowing in the thruster's discharge chamber when tests were attempted at higher background pressure conditions. This was attributed to the fact that thruster bakeout was performed at the lowest possible achievable background pressure at discharge voltages of 600 and 650 V. As such, the erosion band downstream edge was formed based on test conditions at low pressure and high voltage (600 V and above). Attempts to run at artificially elevated background pressures for high voltage operation resulted in the discharge moving upstream towards the anode (as was the case for all other conditions) and causing glowing of the downstream edge of the erosion zone due to ion bombardment. When the erosion zone edge started to glow, that caused the discharge current to rise quickly, and the thruster started to operate unstably. At each test condition in Table 3, the thruster performance was optimized at the lowest facility background pressure condition, those electromagnet settings were preserved when testing at the higher facility background pressure conditions.

Table 3. Thruster test conditions during the facility background pressure sensitivity test at NASA GRC's VF5.

Discharge Voltage, V	Discharge Power, kW	Pressure, Torr
300	1.5	$1.1 \times 10^{-6}$
300	3.0	$1.8 \times 10^{-6}$
400	2.0	$1.2 \times 10^{-6}$
400	3.2	$1.7 \times 10^{-6}$
500	2.0	$1.2 \times 10^{-6}$
500	3.0	$1.7 \times 10^{-6}$
500	3.9	$2.0 \times 10^{-6}$

Figure 11 presents the thruster discharge current for the various test conditions as a function of facility background pressure (log scale). In general, results in Fig. 11 show that increasing the facility background pressure increased the thruster's discharge current. Figure 12 presents thrust magnitudes for the various test conditions as a function of facility background pressure (log scale). In general, results in Fig. 12 show that increasing the facility background pressure increased the thruster's thrust levels. The trends observed in Figs. 11 and 12 are expected since higher facility background pressures result in higher ingested flow and higher discharge current and thrust. However, as discussed earlier, the percentage increase in the thruster's discharge current and thrust at the elevated facility background pressure conditions cannot only be explained by assuming that it is all due to flow ingestion

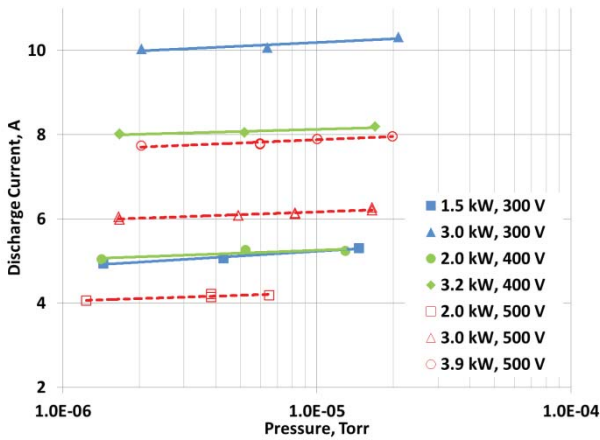


**Figure 11. Discharge current variation as a function of facility background pressure during the pressure sensitivity test at NASA GRC's VF5.**

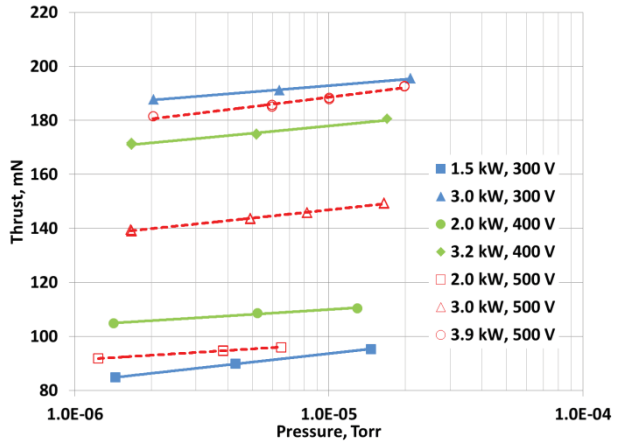


**Figure 12. Thrust variation as a function of facility background pressure during the pressure sensitivity test at NASA GRC's VF5.**

even if we assume that the ingestion area is two or three times greater than the thruster's physical open area due to ionization occurring outside the thruster's exit plane. As stated earlier, there is evidence of the ionization and erosion zones shifting upstream towards the thruster anode as the facility background pressure was increased.

Figures 13 and 14 present the variation of discharge specific impulse and efficiency as a function of facility background pressure. As expected, the trends observed match what was reported in Fig. 12. Both discharge specific impulse and efficiency increase with increased facility background pressure. Table 3 presents the ratio of discharge current, thrust, discharge specific impulse, and discharge efficiency at three and ten times the baseline pressure relative to their values during baseline pressure thruster operation. As was indicated earlier, discharge current and thrust both increased as the facility background pressure was increased. The results in Table 3 indicate that although flow ingestion is contributing to increased xenon flow to the thruster, the increase in the discharge current and thrust magnitudes cannot only be explained by accounting for this additional flow. Discussion of Table 3 results will be presented in Section IV.

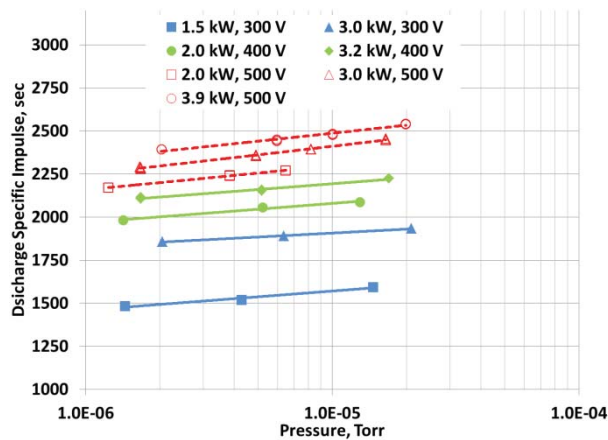


**Figure 13. Discharge specific impulse variation as a function of facility background pressure during the pressure sensitivity test at NASA GRC's VF5.**

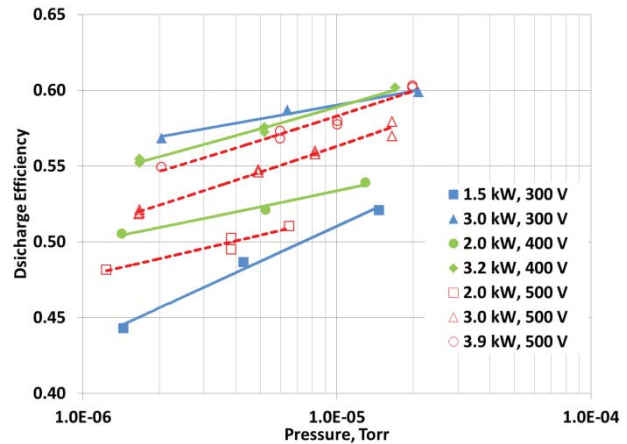


**Figure 14. Discharge efficiency variation as a function of facility background pressure during the pressure sensitivity test at NASA GRC's VF5.**

**Table 3. Ratio of discharge current, thrust, discharge specific impulse, and discharge efficiency relative to values at baseline pressure for thruster operation at 3 (blue) and 10 (red) times the baseline pressure  $P_0$ . Note \* denotes results at  $5 \times P_0$ .**

Test Condition	$3 \times P_0$				$10 \times P_0$			
	$I_d/I_{d0}$	$T/T_0$	$I_{sp}/I_{sp0}$	$\eta/\eta_0$	$I_d/I_{d0}$	$T/T_0$	$I_{sp}/I_{sp0}$	$\eta/\eta_0$
300V 1.5kW	1.02	1.06	1.060	1.10	1.07	1.12	1.12	1.18
300V 3.0kW	1.00	1.02	1.02	1.03	1.03	1.04	1.04	1.05
400V 2.0kW	1.04	1.04	1.04	1.03	1.04	1.05	1.05	1.07
400V 3.2kW	1.00	1.02	1.02	1.04	1.02	1.05	1.05	1.09
500V 2.0kW	1.03	1.03	1.03	1.04	1.03*	1.05*	1.05*	1.06*
500V 3.0kW	1.01	1.03	1.03	1.05	1.03	1.07	1.07	1.10
500V 3.9kW	1.01	1.04	1.04	1.08	1.03	1.08	1.08	1.13

Figure 15 presents the cathode-to-ground voltage ( $V_{c-g}$ ) magnitudes as a function of facility background pressure for the various test conditions. Results indicate, in general, that the  $V_{c-g}$  becomes less negative as the facility background pressure is increased. In addition, results in Fig.15 seem to indicate that change is less profound at higher power thruster operation. For example, at 300 V and 1.5 kW,  $V_{c-g}$  decreases from -19 V to -17.2 V as the facility pressure is increased by a factor of 10. However, at 300 V and 3.0 kW,  $V_{c-g}$  decreases from -9.2 V to -8.6 V as the facility pressure is increased by a factor of 10. A similar trend is observed at a discharge voltage of 500 V. At 500 V and 2.0 kW,  $V_{c-g}$  decreases from -17 V to -14.5 V as the facility pressure is increased by a factor of 10. At 500 V and 3.0 kW,  $V_{c-g}$  decreases from -15 V to -13.5 V as the facility pressure is increased by a factor of 10. Finally, at 500 V and 3.9 kW,  $V_{c-g}$  decreases from -11.8 V to -10.6 V as the facility pressure is increased by a factor of 10. This could be interpreted as an indication that electron mobility is more affected at lower flow rates and lower discharge voltages. A discussion of the experimental results in Section 4 will further elaborate on the results presented in Figs. 11-15 and Table 3.

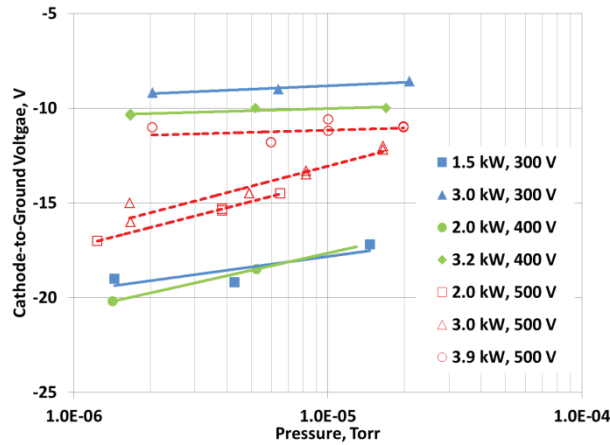


**Figure 15. Cathode-to-ground voltage variation as a function of facility background pressure during the pressure sensitivity test at NASA GRC's VF5.**

### B.3 Voltage-Current Characterization

The V-I profiles of the HiVHAc EDU thruster were obtained for various thruster flow rates and electromagnet settings at different facility background pressures. These characteristics were measured to assess how the thruster operation and stability is affected by operation at elevated background pressure conditions.

The HiVHAc EDU thruster V-I characterization was acquired for anode flow rates of 2, 3, 4, 5, 6, 6.5, and 7 mg/s for electromagnet currents magnitudes of  $I_o$ ,  $1.5 \cdot I_o$ , and  $2 \cdot I_o$ . For all test conditions, the thruster discharge voltage was varied between 200 and 600 V at 1 V increments with a voltage ramp rate of 1V/s. During the V-I characterization tests, a 15 kW high voltage power supply capable of 600 V was used. Control software programmed by the Aerospace Corp. was used to perform and record the V-I profiles of the thruster.

The thruster V-I profiles provide insights into thruster behavior and stability under different electromagnet settings. The V-I profiles presented in Figs. 16 through 23 have four distinct regions and trends and they are:

- A negative sloped region where as the discharge voltage is increased the discharge current decreases (negative impedance); in this region it was observed that the thruster discharge current oscillations were large;
- A flat region where as the discharge voltage is increased the discharge current, for the most part, was unchanged; this region was characterized by relatively small discharge current oscillations and is desirable;
- A positive sloped region where as the discharge voltage is increased the discharge current increases (positive impedance); in this region the discharge current oscillations magnitude was relatively greater than the flat region but was less than their magnitude in the negative region; and
- A hump region where the discharge current increases rapidly with the discharge voltage in a narrow voltage region, this typically resulted in large magnitude discharge current oscillations.

The thruster V-I profiles for flow rates between 6 and 7 mg/s were obtained for elevated pressure conditions that were only 3 times the lowest attainable condition. Tests at 10 times the baseline pressure condition resulted in the thruster operating unstably and the discharge current magnitudes increasing dramatically. Also at flow rates between 6 and 7 mg/s, V-I profiles were only acquired for electromagnet currents of  $1.5 \cdot I_o$  and  $2 \cdot I_o$ , tests at  $I_o$  resulted in unstable thruster operation at elevated background pressure conditions.

Discussion of the V-I profiles for operation at the baseline pressure conditions were presented in Ref. 9, the discussion herein focuses on the change in the V-I profiles as a result of elevating the facility background pressure to three and ten times the baseline (lowest achievable) value. Note that in Figs. 16-23, P1 refers to the baseline pressure condition, P2 refers to pressures that are three times the baseline value P1, and P3 refers to pressures that are approximately ten times the baseline value of P1.

Figures 16-18 present the V-I profiles for anode flow rates of 2, 3, and 4 mg/s, Figs. 16-18 indicate similar characteristics. Increasing the facility background pressure increased the discharge current magnitude, and that increase became more pronounced at P3. The thruster still operated stably for the entire voltage range of 200-600 V but with elevated discharge current and reduced performance.

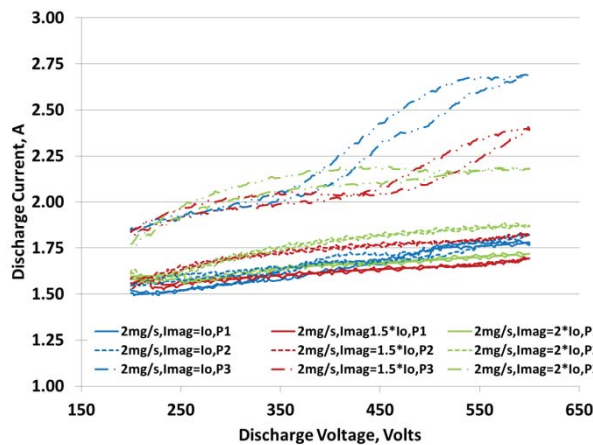


Figure 16. V-I profiles for anode flow rate of 2 mg/s at facility background pressure of P1, P2, and P3 for electromagnet settings of  $I_o$ ,  $1.5 \cdot I_o$ , and  $2 \cdot I_o$ .

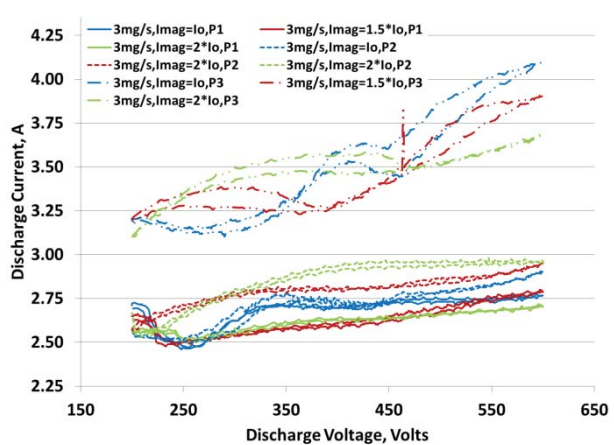
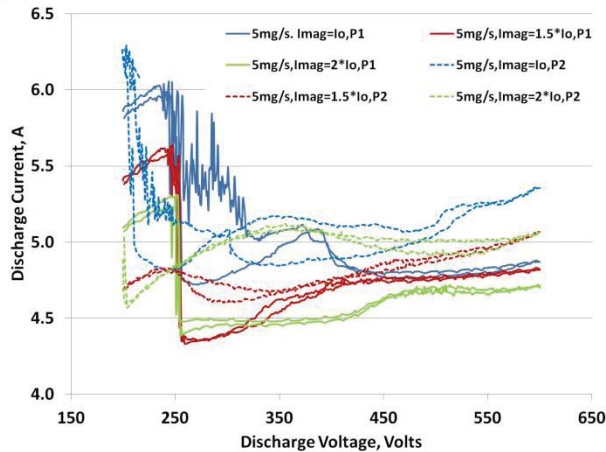


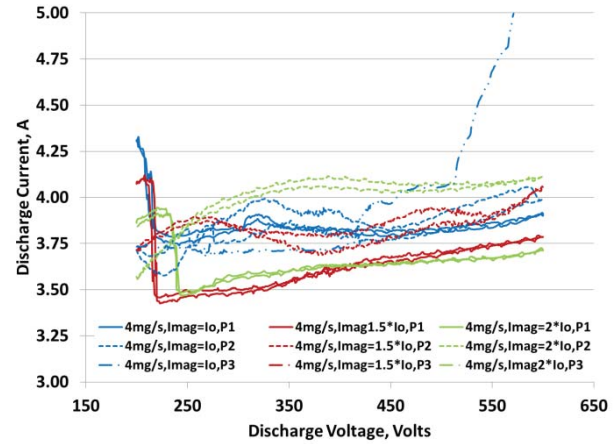
Figure 17. V-I profiles for anode flow rate of 3 mg/s at facility background pressure of P1, P2, and P3 for electromagnet settings of  $I_o$ ,  $1.5 \cdot I_o$ , and  $2 \cdot I_o$ .



Figure 19 presents the V-I profiles for 5 mg/s for P1 and P2 only, thruster operation at P3 was not attainable due to a dramatic increase in the discharge current and large peak-to-peak discharge current oscillations. At 5 mg/s thruster operation, increasing the facility background pressure from P1 to P2 (3 times P1) caused the V-I profiles to shift up (higher discharge currents at a given discharge voltage). This is similar to what was observed in Figs. 16-18. Figure 20 presents the V-I profiles for 5 mg/s after allowing the thruster to reach steady state thermal conditions, referred to as hot. Profiles in Fig. 20 show that for the most part, the initial and hot profiles look very similar except for the  $2 \cdot I_0$  profile with the difference being at discharge voltages between 200 and 450 V.



**Figure 19.** V-I profiles for anode flow rate of 5 mg/s at facility background pressure of P1, and P2 for electromagnet settings of  $I_0$ ,  $1.5 \cdot I_0$ , and  $2 \cdot I_0$ .



**Figure 18.** V-I profiles for anode flow rate of 4 mg/s at facility background pressure of P1, P2, and P3 for electromagnet settings of  $I_0$ ,  $1.5 \cdot I_0$ , and  $2 \cdot I_0$ .

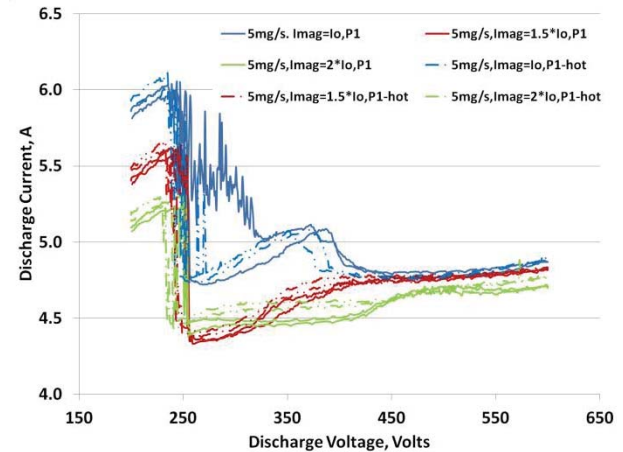


**Figure 20.** V-I profiles for anode flow rate of 5 mg/s at facility background pressure of P1 for electromagnet settings of  $I_0$ ,  $1.5 \cdot I_0$ , and  $2 \cdot I_0$  for thruster operation at steady state thermal conditions.

Figures 21-23 present the V-I profiles for 6, 6.5, and 7 mg/s for P1 and P2 only. Thruster operation at P3 was not attainable due to a dramatic increase in the discharge current and large peak-to-peak discharge current oscillations. In addition, V-I profiles at  $I_0$  and P1 were not attainable due to unstable thruster operation,<sup>9</sup> however, at P2 thruster operation at  $I_0$  was realized and is presented in Figs. 21-23. Similar to the V-I characteristics at flow rates of 2-5 mg/s, the V-I characteristics at 6-7 mg/s indicate that the HiVHAc EDU thruster operates differently as the facility background pressure is modestly increased from P1 to P3.

In summary, the HiVHAc EDU thruster V-I profiles and characteristics suggest and indicate that increasing the VF5 facility background pressure by a factor of 3 above the lowest attainable pressure at all anode flow rates and electromagnet settings, resulted in the V-I profiles changing features. That change was more pronounced at higher discharge voltages.

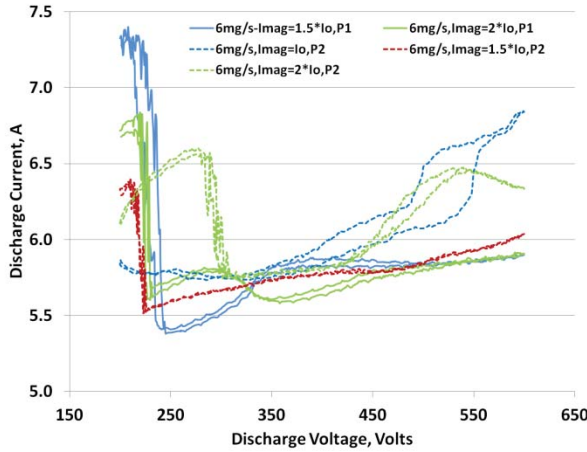


**Figure 21. V-I profiles for anode flow rate of 6 mg/s at facility background pressure of P1, and P2 for electromagnet settings of  $I_o$ ,  $1.5 \cdot I_o$ , and  $2 \cdot I_o$ .**

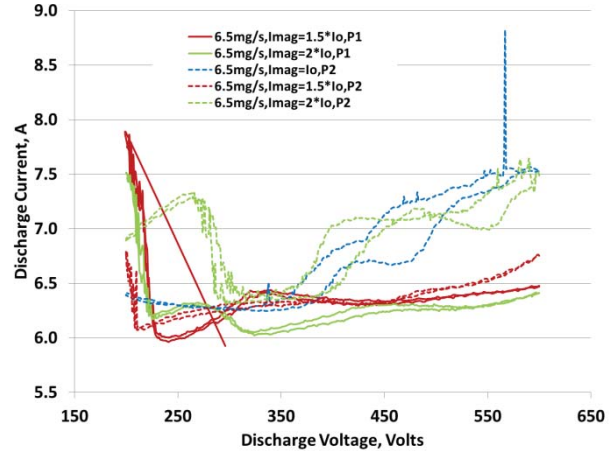


**Figure 22. V-I profiles for anode flow rate of 6.5 mg/s at facility background pressure of P1 and P2 for electromagnet settings of  $I_o$ ,  $1.5 \cdot I_o$ , and  $2 \cdot I_o$ .**

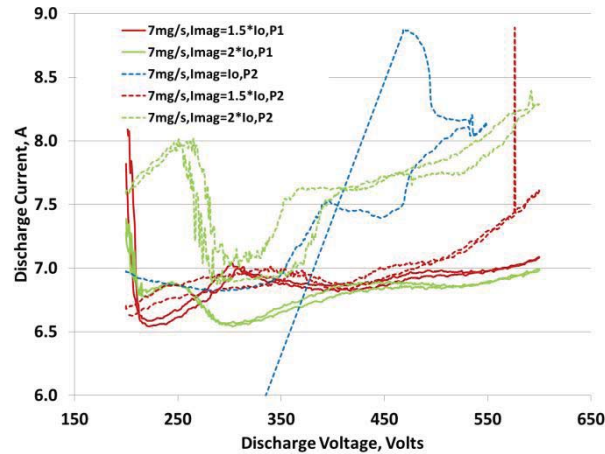


**Figure 23. V-I profiles for anode flow rate of 7 mg/s at facility background pressure of P1 and P2, for electromagnet settings of  $I_o$ ,  $1.5 \cdot I_o$ , and  $2 \cdot I_o$ .**

## IV. Discussion

Variations in the facility background pressure affected the thruster's discharge current, thrust, and V-I characteristics. For all test conditions, the thruster had a higher discharge efficiency and discharge specific impulse for the higher background pressure conditions. Figure 24 shows photographs of the thruster operating at a discharge voltage of 400 V and 2.4 kW at background pressure conditions of three, ten, and twenty four times the baseline value. This increased thruster performance, due to elevated background pressure magnitudes, cannot only be attributed to flow ingestion since at the highest background pressure condition (P3) the ingested flow only contributes an additional 0.3-0.5% to the total injected flow. Photographs in Fig. 24 clearly show that the coupling between the cathode and thruster discharge and the thruster plume structure are changing as the facility background pressure is increased. The plasma bridge between the cathode and discharge is becoming more luminous and pronounced, and the thruster's plume is becoming more diffuse as the background pressure is increased. In addition, there is experimental evidence that increasing the facility background pressure caused the thruster's discharge to shift upstream towards the thruster's anode. This observation is supported by the fact that attempts to operate the thruster at discharge voltages of 600 and 650 V and elevated facility background magnitudes were not successful

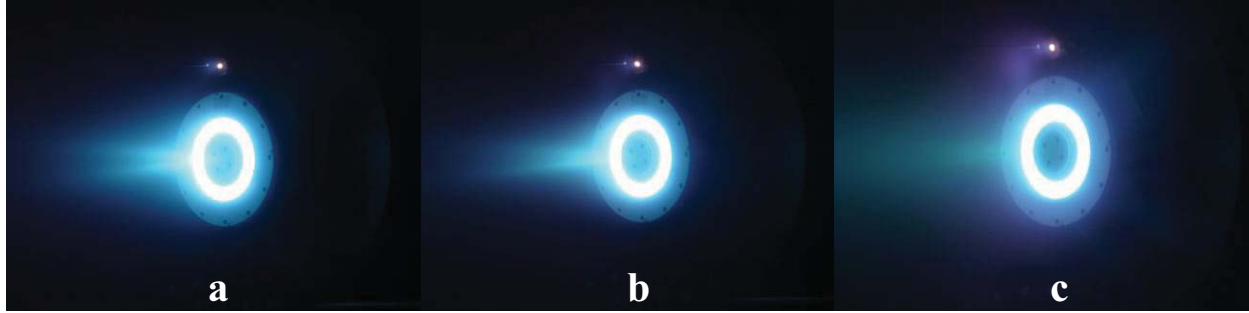


**Figure 24. Photograph of the HiVHAc EDU 2 thruster operating at three (a), ten (b), and 24 (c) times lowest attainable facility background pressure.**

due to the discharge moving upstream towards the anode and causing glowing of the erosion zone downstream end as described earlier in this paper. Another supporting fact was that thermocouples attached to the inner and outer boron nitride discharge channel walls downstream end recorded an increase in temperature as VF5 background pressure was increased, this supports our claim that the discharge moved upstream towards the anode.

Results in Table 3 and Figs. 11-15 indicate that at a discharge voltage of 300 V, the relative increase in the operating discharge current and thrust was higher for 1.5 kW than 3 kW operation. This may indicate that, at a given discharge voltage, lower power operation results in lower neutral density in the discharge chamber and thruster exit region, and the thruster operation is then more sensitive to the local background pressure magnitude when compared to higher flow operating conditions. Results in Table 1 for 400 and 500 V operation, indicate that in general the relative increase in the discharge current at lower power operation was higher than at higher power operation although the relative increase was not as pronounced for 300 V operation.

A study by Huang *et al.*<sup>16</sup> used Faraday,  $E \times B$ , and retarding potential analyzer probes to gain insights to help us understand how increasing the facility background pressure affects thruster operation and performance. The various probe data is used to estimate thruster discharge efficiency by use of a phenomenological efficiency model. The model used in this paper is the same as a prior work by Shastri,<sup>19</sup>

$$(\eta_t)_d = \eta_v \eta_d \eta_b \eta_m \eta_q \quad (5)$$

Where  $\eta_v$  is the voltage utilization efficiency,  $\eta_d$  is the divergence efficiency,  $\eta_b$  is current utilization efficiency,  $\eta_m$  is the mass utilization efficiency,  $\eta_q$  is the charge utilization efficiency. As such the phenomenological efficiency model provides insights that help in assessing the various loss mechanisms during Hall thruster operation. A detailed analysis of the far-field probe data was performed by Huang. *et al.*<sup>16</sup>, and the plume study revealed that increasing the facility background pressure resulted in changes to how the HiVHAc EDU thruster was operating. The study found that increased background pressure resulted in the average charge state rising rapidly and then leveling off with rising background pressure. At the same time the study found that the thruster's plume divergence and ion beam (as computed by integrating the ion beam profiles) decreased with increased background pressure. The average energy per charge fell with increased facility background pressure. As such, the various plasma probes are indicating that increase facility background pressure is causing a fundamental change in the thruster operation.

The findings from this study and the study by Huang *et al.*<sup>16</sup> indicate that a complex interrelated change in the HiVHAc EDU operation occurred as the facility background pressure was increased. As would be expected the thruster performance increased, but the region of stable high-performance operation narrowed with increasing facility pressure. Previous studies on facility effects by Mitchell<sup>20</sup> and Azziz<sup>21</sup> also indicated that plume ingestion does not fully account for the change in thruster performance due to variations in the facility background pressure, but a more complex interaction may be occurring that results in changes to the discharge location and changes in the coupling between the discharge and the cathode.

## V. Conclusion and Future Work

This study was a first step towards gaining a better understanding of how facility background pressure affects and impacts the HiVHAc EDU thruster performance and stability. An extensive performance evaluation of the HiVHAc EDU thruster was undertaken at NASA GRC's VF5. The objective of this study was to test the thruster in the lowest attainable background pressure environment. VF5 test results indicated thruster performance levels that were lower than that measured in VF12 during the thruster's performance acceptance tests. Additional tests were performed in VF5 at selected thruster operating conditions to investigate and elucidate the underlying physics that changed during thruster operation as the facility background pressure was increased. Test results found that flow ingestion does not account entirely for the change in thruster performance at the elevated background pressure levels even if we assume that the ingestion area is two or three times greater than the thruster's physical open area due to ionization occurring outside the thruster's exit plane. Experimental results indicated that the cathode-to-ground voltage magnitudes changed as the facility background pressure was varied. This indicated that the coupling between the cathode and thruster's discharge was changing. The thruster's V-I profiles results indicated that the region of stable thruster operation narrowed as the facility background pressure was increased. Experimental evidence that the ionization and acceleration zones were shifting upstream towards the thruster's anode were also observed in this test series. Plasma probe results also confirmed that flow ingestion does not explain or account for the entire change in thruster performance and operating characteristics as the facility background pressure was increased.<sup>16</sup> A set of near-field high speed Langmuir probe and FAST camera measurements have been analyzed. Data from the two diagnostics suggest that the ionization and acceleration zones of the thruster were shortening and receding into the discharge chamber as was suggested earlier from test observations. Data from FAST camera measurements also indicate that the oscillation frequency of the breathing mode rises with background pressure.<sup>18</sup> Analysis of IR camera and thermocouple measurements is on-going and the additional data set will further elucidate and clarify how operation at elevated facility background pressure impacted thermal operating characteristics of the HiVHAc thruster.

Future plans will entail additional VF5 tests of the HiVHAc EDU thruster at even lower background pressure conditions. VF5 has recently undergone facility improvements that resulted in background pressure magnitudes that are at least two to three times lower than what was achieved in this test campaign. Additional tests of the HiVHAc thruster will be performed in FY15, the tests will include:

- Performance characterization at facility background pressure of approximately  $1 \times 10^{-6}$  Torr during full power thruster operation;
- Performance characterization at constant power;
- V-I characterization;
- Thermal characterization using thermocouples and an IR camera;
- Plume characterization using faraday,  $E \times B$ , and retarding potential analyzer probes;
- FAST camera measurements of the thruster operating modes;
- Inner and outer discharge channel surface Langmuir probe measurements to help ascertain the location of the discharge ionization and acceleration zones;
- Pressure sensitivity study that will employ the full diagnostics suite listed above;
- Investigation of cathode position and cathode flow fraction variation on thruster performance; and
- Investigation of impact of magnetic circuit topology on thruster operation at various facility background pressure levels.

The ultimate objective of this upcoming pressure characterization investigation is to determine the "appropriate" facility background pressure that best simulates operation in space and then use the investigation findings to better quantify how operation at different facilities and at higher facility background pressure changes the performance, plume structure, stability, discharge characteristics, and erosion rates of the HiVHAc EDU thruster. This is critical in the development of the HiVHAc thruster since wear testing of the thruster will be performed in VF12 which is not capable of attaining the same facility background pressure levels as VF5.

## Acknowledgments

The authors would like to thank and acknowledge the Science Mission Directorate for funding this work. The authors also acknowledge the contributions of Aerojet-Rocketdyne, Colorado Power Electronics, and VACCO in helping develop and manufacture the HiVHAc system components. Lastly, the authors thank Kevin Blake, George Jacynycz, Michael McVetta, and James Mullins for helping assemble and install the thruster in the vacuum facility, as well as maintaining and operating the vacuum facility.



## References

- <sup>1</sup> Sovey, J. S., Rawlin, V. K., and Patterson, M. J., "Ion Propulsion Development Projects in U.S.: Space Electric Rocket Test to Deep Space 1," *Journal of Propulsion and Power*, Vol. 17, No. 3, May-June 2001, pp. 517-526.
- <sup>2</sup> Russel, C. T., *et al.*, "Dawn: A Journey to the Beginning of the Solar System," DLR International Conference on Asteroids, Comets, and Meteors, July-August 2002.
- <sup>3</sup> Garner, C.E., Rayman, M.D., and Brophy, J.R., "In-Flight Operation of the Dawn Ion Propulsion System Through Year One of the Cruise to Ceres," AIAA-2013-4112, July 2013.
- <sup>4</sup> NASA's Science Mission Directorate Science Plan for 2007-2016.
- <sup>5</sup> Dankanich, J. W., "Electric Propulsion for Small Body Missions", AIAA Paper 2010-6614, August 2010.
- <sup>6</sup> Anderson, D. J., Munk, M., Pencil, E., Dankanich, J., Glaab, L., and Peterson, T., "The Status of Spacecraft Bus and Platform Technology Development under the NASA ISPT Program," IEEEAC Paper #2138, 2013 IEEE Aerospace Conference, Big Sky, MT, March 2-9, 2013
- <sup>7</sup> Shastry, R., Herman, D. A., Soulas, G. C. and Patterson, M. J., "Status of NASA's Evolutionary Xenon Thruster (NEXT) Long-Duration Test as of 50,000 h and 900 kg Throughput," 33<sup>rd</sup> International Electric Propulsion Conference, IEPC-2013-121, Washington D.C., 6-10 Oct, 2013.
- <sup>8</sup> Dankanich, J.W., Drexler, J. A., and Oleson, S. R., "Electric Propulsion Mission Viability with the Discovery-Class Cost Cap," AIAA Paper 2010-6776, August 2010.
- <sup>9</sup> Kamhawi, H., Haag, T., Huang, W., Pinero, L., Peterson, T., and Dankanich, J., "Integration Tests of the High Voltage Hall Accelerator System Components at NASA Glenn Research Center," 33<sup>rd</sup> International Electric Propulsion Conference, IEPC-2013-445, Washington, DC, 6-10 Oct., 2013.
- <sup>10</sup> Byers, D., and Dankanich, J., "A Review of Facility Effects on Hall Effect Thrusters," 31st International Electric Propulsion Conference, IEPC-2009-076, Ann Arbor, MI, Sep., 2009.
- <sup>11</sup> Randolph, T., *et al.*, "Facility Effects on Stationary Plasma Thruster Testing", 23rd International Electric Propulsion Conference, IEPC-1993-093, Seattle, WA, Sep., 1993.
- <sup>12</sup> Diamant, K. D., Spektor, R., Beiting, E. J., Young, J. A., and Curtiss, T. J., "The Effects of Background Pressure on Hall Thruster Operation", *48th AIAA/ASME/SAE/ASEE Joint Propulsion Conference & Exhibit*, AIAA-2012-3735, Atlanta, GA, 29 Jul.- 1 Aug., 2012.
- <sup>13</sup> Kamhawi, H., *et al.*, "Performance and Environmental Test Results of the High Voltage Hall Accelerator Engineering Development Unit," AIAA 2012-3854, July 2012.
- <sup>14</sup> Pinero, L. R., Kamhawi, H., and Drummond, G., "Integration Testing of a Modular Discharge Supply for NASA's High Voltage Hall Accelerator Thruster," IEPC Paper 2009-275, September 2009.
- <sup>15</sup> Hesterman, B., "Wide Range Multi-Phase Resonant Converters," JANNAF-1435, May 2010.
- <sup>16</sup> Huang, W., Kamhawi, H., and Haag, T., "Effect of Background Pressure on the Performance and Plume of the HiVHAc Hall Thruster", 33rd International Electric Propulsion Conference, IEPC-2013-058, Washington, DC, 6-10 Oct, 2013.
- <sup>17</sup> Lobbia, R. B., "A Time-resolved Investigation of the Hall Thruster Breathing Mode," Ph.D. Dissertation, Aerospace Engineering, University of Michigan, Ann Arbor, MI, 2010.
- <sup>18</sup> Huang, W., H., Kamhawi, H., Lobbia, R. B., and Brown, D. L., "Effect of Background Pressure on the Plasma Oscillation Characteristics of the HiVHAc Hall Thruster," 50th AIAA/ASME/SAE/ASEE Joint Propulsion Conference, Cleveland, OH, July 28-30, 2014.
- <sup>19</sup> Shastry, R., Hofer, R. R., Reid, B. M., and Gallimore, A. D., "Method for analyzing ExB probe spectra from Hall thruster plumes", *Review of Scientific Instruments*, Vol. 80, No. 6, doi:10.1063/1.3152218, 22 Jun., 2009, pp. 063502.
- <sup>20</sup> Walker, M. L. R., "Effects of Facility Backpressure on the Performance and Plume of a Hall Thruster," Ph.D. Dissertation, Aerospace Engineering, University of Michigan, Ann Arbor, MI, 2005.
- <sup>21</sup> Azziz, Y., and Martinez-Sanchez, M., "Experimental and Theoretical Characterization of a Hall Thruster Plume," Ph.D. Dissertation, Department of Aeronautics and Astronautics, Massachusetts Institute of Technology, Cambridge, MA, 2007.